Sci Eng Compos Mater 18 (2011): 167–171 © 2011 by Walter de Gruyter • Berlin • Boston. DOI 10.1515/SECM.2011.027

Fabrication and characterization of unidirectional CF/Al composites

Moonhee Lee*, Yongbum Choi, Kenjiro Sugio, Kazuhiro Matsugi and Gen Sasaki

Department of Mechanical Science and Engineering, Graduate School of Engineering, Hiroshima University, 1-4-1 Kagamiyama, Higashi-Hiroshima 739-8527, Japan, e-mail: leemoonhee@hiroshima-u.ac.jp

*Corresponding author

Abstract

The unidirectional carbon fiber (CF) reinforced aluminum (Al) composites have been fabricated by the low pressure infiltration (LPI) of molten Al into porous CF preform. Prior to the fabrication of the unidirectional CF/Al composites, the unidirectional CF preform was prepared by sintering of CFs and copper (Cu) particles under the spark plasma sintering (SPS). The compression strength of CF preform was examined to determine the infiltration pressure of molten Al into CF preform. The effects of the different infiltration pressures and sizes of Cu particles on the densification of unidirectional CF/Al composites have also been investigated. The compression strength of CF preform increased with increasing of the contact area between CFs and Cu particles. The density of CF/Al compo sites improved with the increase of the infiltration pressure. The CF/Al composites, into which the bimodal Cu particles are added, have average particle sizes of 2.55 μm and 11.79 μm, with a high relative density of about 95% with the nearly homogeneous fiber distribution.

Keywords: CF/A1 composites; carbon fiber preform; low pressure infiltration; fiber distribution.

1. Introduction

Recently, the high performance thermal management materials have been developed in accordance with development of high heat generation electronic components. Especially, the thermal dissipation ability of heatsink materials on electronic components, including semiconductors, light emitting diodes (LED) and converter modules is key issue in accordance with the development of the hybrid electric vehicles (HEV) and electric vehicles (EV) [1–5]. In the meantime, the composite materials have been one of the candidate materials with excellent advantages, such as, high thermal conductivity (TC), coefficient of thermal expansion (CTE) matching, light weight and net shape fabrication [6, 7].

In the thermal management industry, SiC/Al and diamond/Cu composites with high TC, have been investigated in terms of CTE matching and high thermal conductivity [8, 9]. However, these materials have difficulty in machining with high hardness of their reinforcements. On the other hand, CF/Al composites are expected to represent, not only easy to machine, but also high TC in accordance with the development of the high TC carbon fibers.

The casting processes for metal matrix composite materials are widely divided into squeeze casting and a low-pressure infiltration (LPI) process. Those casting processes are differentiated by applied infiltration pressure of molten metal into porous preform. The squeeze casting process for fabrication of fiber reinforced composite materials has caused fiber fracture and/or inhomogeneous fiber distribution by high applied pressure [10, 11], whereas the LPI process has applied approximately atmospheric pressure. Therefore, LPI process for the composite materials enabled relatively simple facilities and cost-effective and complex shape fabrication using low applied pressure [12, 13]. In addition, optimization of the fabrication process for the fiber preform, as well as composite materials, came to be needed in order to obtain high performance composite materials.

In this study, the CF preform and CF/Al composites were fabricated by the spark plasma sintering (SPS) process and LPI process, respectively. Compression tests on the CF preform were carried out to characterize the strength of CF preforms fabricated with different temperature conditions. Furthermore, the influences of applied infiltration pressure and homogeneity of fiber distribution on the densification of CF/Al composites have been discussed.

2. Experimental procedure

The unidirectional CF preform was fabricated by sintering of the unidirectional CF mixtures. The CF mixtures were prepared by blending with 30 vol% of coal tar pitch based K13D2U carbon fibers (Mitsubishi Plastics, Inc., Tokyo, Japan), 10 vol% of atomized Cu powder (Fukuda Metal, Foil & Powder Co, LTD, Kyoto, Japan) and polyethylene glycol (PEG) as a dispersant. The Cu powders were dispersed into the CF bundles by passing CF mixtures through a graphite roller and play a role such as spacing and bridging between CFs. The Cu powders added with different particle size conditions, are shown in Table 1. The CF mixtures were put into the cylindrical graphite mold and sintered under the SPS process by the electrical direct current discharge into the CF mixtures under a vacuum of 2.7×10^{-2} Pa. The sintering conditions for CF preform by the SPS process were sintering temperatures

Table 1 Various kinds of Cu powders for fabrication of carbon fiber preform.

Products	Cu HWQ -5 µm ①	Cu HWQ -20 µm with 20 µm sieving ②	①+② (①:②=50%:50%)	Hukuda Metal 25~45 µm
Fabrication process	Atomization			Eletrolysis
Average particle size (µm)	2.55	11.79	Bimodal	28.86
Volume fraction (%)	10			

of 800, 850 and 900°C in accordance with the applied electrical current and voltage of 380 A/4 V, 390 A/4 V and 410 A/4 V, respectively. The temperature was directly measured at the center of the graphite mold. On the other hand, another CF preform as a reference material was also fabricated by the high temperature sintering process in the electrical furnace at 850°C under vacuum.

Subsequently, CF/Al composites were fabricated under the LPI process by means of the infiltration of molten Al (A1070) into porous CF preform. The infiltration pressure and temperature conditions of LPI process were 0.2–0.8 MPa and 800°C under Ar atmosphere. The dimension of CF preform and CF/Al composites was diameter10×L 10 mm^3 in and length. The compression test on the CF preform was carried out to characterize the strength property by universal test machine (Shimadzu Corp., Kyoto, Japan). The crosshead speed for the compression test was 0.5 mm/min at room temperature. The microstructure of both materials was observed by scanning electron microscopy. The density of CF/Al composites was measured by Archimedes' technique.

3. Results and discussion

In order to examine the sintering phenomenon on Cu particles in CF preform, Figure 1 represents the microstructures of CF preforms with different fabrication processes such as the high temperature sintering process [Figure 1(A)] and SPS process [Figure 1(B)] at the fabrication temperature of 1123 K. The average Cu particle size of 2.55 µm was utilized for the fabrication of CF preforms in this experiment. The Cu particles were distributed to maintain some space between CFs. The adequate spaces between CFs are expected to facilitate the infiltration of molten Al into CF preform. However, Figure 1(A) shows only weak bonding between Cu-Cu and CF-Cu contacts by sintering temperature lower than the Cu melting point of 1356 K. Meanwhile, Figure 1(B) shows not only Cu particle bonding and bridging CFs, but also deposition of Cu particles on the CF surfaces. It was reported that the melt and vaporization of metal powders occurred under the SPS process by means of the locally high heat generation attained by concentration of the electrical current density at the points of powder contacts [14, 15]. The coalescence of Cu particles between CFs and deposition of Cu particles on CFs in this study might take place by the melting and vaporization of Cu particles, even if the measured sintering temperature at the graphite mold was lower than the melting point of Cu. The formation of the Cu bridging between CFs by SPS process can be expected to improve the strength property of CF preform. Especially, the effect of the CF-Cu contact size by Cu bridging on compression strength of CF preform was examined.

The relationship between compression strength and CF-Cu contact area of the CF preforms is shown in Figure 2 by normalized plots, depending on the fabrication temperatures ranging from 1073 K to 1173K. The compression strength and CF-Cu contact area of CF preform increased with increasing fabrication temperature. The compression strength and contact area at the sintering temperature of 1173 K showed 2.15 MPa and 10.81 μm^2, which corresponds to about 2.1 and 3.6 times higher value than that of 1073 K. In other words, the compression strength of the CF preform was significantly affected by the size of contact area between Cu bridging and CFs. In order to fabricate the CF/Al composites by the LPI process, the infiltration pressure of molten Al into CF preform must be determined according to the compression strength of CF preform.

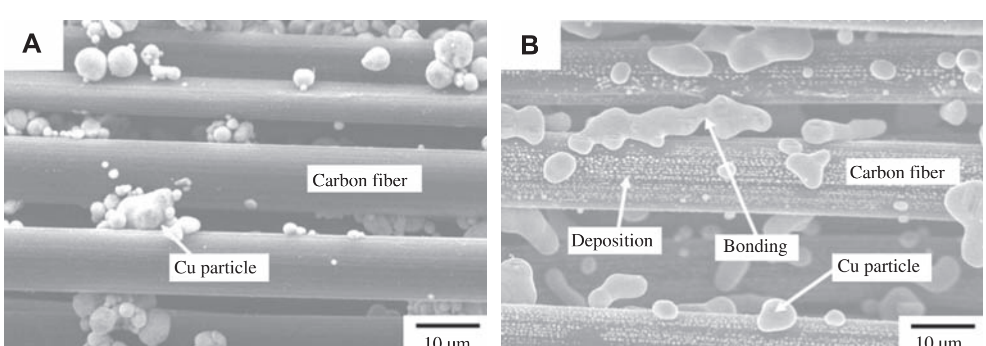

Figure 1 Microstructure of CF preform with different fabrication methods; (A) high temperature sintering process and (B) the SPS sintering at their fabrication temperatures of 850°C.

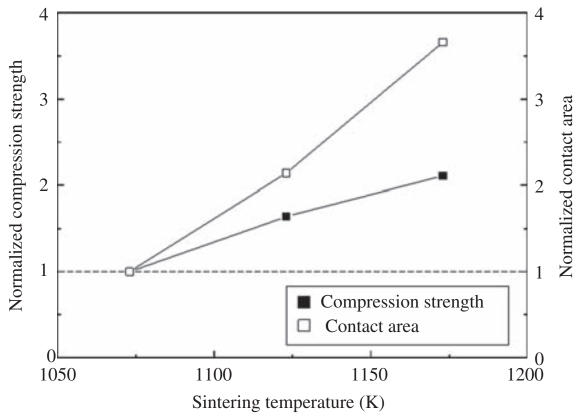

Figure 2 Effect of fabrication temperature on compression strength of CF preform and CF-Cu contact area.

The CF/Al composites were fabricated with the infiltration of the molten Al into the longitudinal fiber direction of the CF preform by direct loading of the infiltration pressures. The density of CF/Al composites was significantly affected by the applied infiltration pressure, as shown in Figure 3 (A). The average Cu particle size of 12.44 µm was used for the CF preform in this experiment. The density of CF/Al compo sites were 1.4, 2.4, 2.6 and 2.66 Mg/m^3 in accordance with the applied pressure of 0.2, 0.4, 0.6 and 0.8 MPa, respectively. Especially, the density of CF/Al composites significantly increased between the infiltration pressures of 0.2 and 0.4 MPa. From the viewpoint of decision on infiltration pressure, the infiltration of melt into unidirectional fiber arrays is mainly influenced by the capillary resistance, internal viscous friction, gravity and back pressure [16, 17]. The molten metal infiltration into the fiber arrays starts when the applied pressure overcomes the threshold pressure of melt infiltration. In the case of the CF volume fraction of 0.3, the threshold pressure to start infiltration of molten Al was calculated to be about 0.2 MPa. In other words, the applied infiltration pressure which exceeded the threshold pressure, facilitated the permeation of molten Al into CF arrays and raised the density of CF/Al composites. However, the CF/Al composites with an applied pressure of 0.8 MPa showed only 84% relative density with the formation of some pores, as shown in Figure 3(B). Most of pores were formed between the clustered CFs in the microstructure. Consequently, the irregular fiber distribution, such as fiber clustering, led to forming of narrow spaces, making it difficult to infiltrate the molten Al between CFs. Therefore, the homogeneous fiber distribution is one of the important parameters to improve the densification of CF/Al composites. In order to form homogeneous fiber distribution, the suitable size of Cu particles as a spacer has to be determined.

Long et al. [16] reported the geometrical description and equations [Eq. (1) and (3)] for the theoretical fiber array. It was known that the space between theoretical fiber arrays was influenced by the volume fraction and radius of fibers. The geometrical schematics based on reference [16] were considered in Figure 4, in order to calculate the theoretical size of a spacer between fibers for the homogeneous fiber distribution. The theoretical size of spacer for the homogeneous square and hexagonal fiber array can be calculated by following equations.

For square fiber array:

$$a=\sqrt{\frac{\pi}{V_f}}R_f \tag{1}$$

$$D=c\text{-}2R_f=\sqrt{2}a\text{-}2R_f \tag{2}$$

For hexagonal fiber array:

$$a=\left(\frac{2\pi}{\sqrt{3}V_f}\right)^{1/2}R_f \tag{3}$$

$$D=2R=2(b\text{-}R_f)=2\left(\frac{a/2}{\cos\ 30^\circ}\text{-}R_f\right) \tag{4}$$

where a, b and c are the distance between each center of adjacent CFs, Cu and CF and distant CFs, D and R are theoretical diameter and radius of Cu, R_f and V_f are radius and volume fraction of CF.

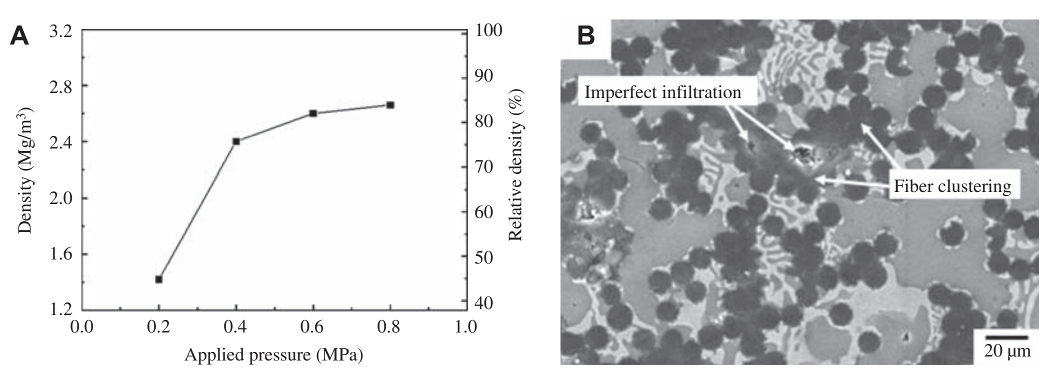

Figure 3 Influence of applied infiltration pressures on CF/Al composites; (A) density variation and (B) microstructure CF/Al composites at 0.8MPa.

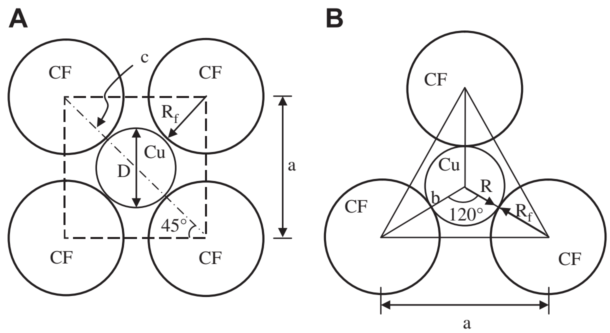

Figure 4 Schemes of theoretical fiber array [16] with Cu spacer for; (A) square fiber distribution and (B) hexagonal fiber distribution.

In the present study, the D were calculated to be about 14.17 and 11.08 μm for the homogeneous square and hexagonal fiber array when the V_f and R_f were 0.3 and 5.5 μm, respectively.

The influence of added Cu particle sizes on the microstructure of CF/Al composites is shown in Figure 5. The applied infiltration pressure for the fabrication of CF/Al composites was 0.8 MPa. In the case of Figure 5(A), the microstructure of CF/Al composites shows both the CF clustering and the large spaces in the matrix. It was supposed that the addition of the 2.55 μm Cu particle, smaller than the theoretical size for homogeneous fiber array, might generate large extra spaces between CFs. As a result, the molten Al infiltrated preferentially into those large spaces with a low volume fraction of fibers during the LPI process. Besides, the molten Al was hard to infiltrate into the narrow spaces with high volume fraction between clustered fibers, even if there existed Cu particles. The narrow spaces became pores because they were too narrow to infiltrate the molten Al with applied infiltration pressure of 0.8 MPa. Figure 5(B) also shows the non-uniform fiber distribution such as fiber clustering and large space of matrix region. It was assumed that 28.86 μm Cu particles, relatively larger than theoretical size, were dispersed locally into the CF fibers and enlarged the space between the fibers. Most of the molten Al infiltrated into the large space between fibers, whereas the narrow space between clustered fibers remained pores, as shown in Figure 5(A). It was reported in [18] that a smaller or larger particle size than the theoretical size has an adverse effect on homogeneity of the fiber distribution. On the other hand, Figure 5(C) shows well dispersed fiber array in comparison with Figures 5(A) and (B). Since the added Cu particles, which had 11.79 μm diameters, were close to the theoretical size, the homogeneity of fiber arrays improved with the decrease of fiber clusters. However, some imperfect infiltration regions were observed in the closed fiber arrays without Cu spacers. In case of Figure 5(D), CF/Al composite shows a nearly homogeneous fiber array without fiber clustering and infiltration defects, mostly by the addition of bimodal Cu particles with average particle sizes of 2.55 μm and 11.79 μm. The added small particles of 2.55 μm might have acted as spacers to prevent the formation of fiber clustering. The CF/Al composites of Figure 5(D) were expected to exhibit excellent mechanical properties without referred defects in the microstructure.

Figure 6 represents the influence of the addition of various Cu particles sizes for the fabrication of CF preform on the density of CF/Al composites. The densities of CF/Al composites

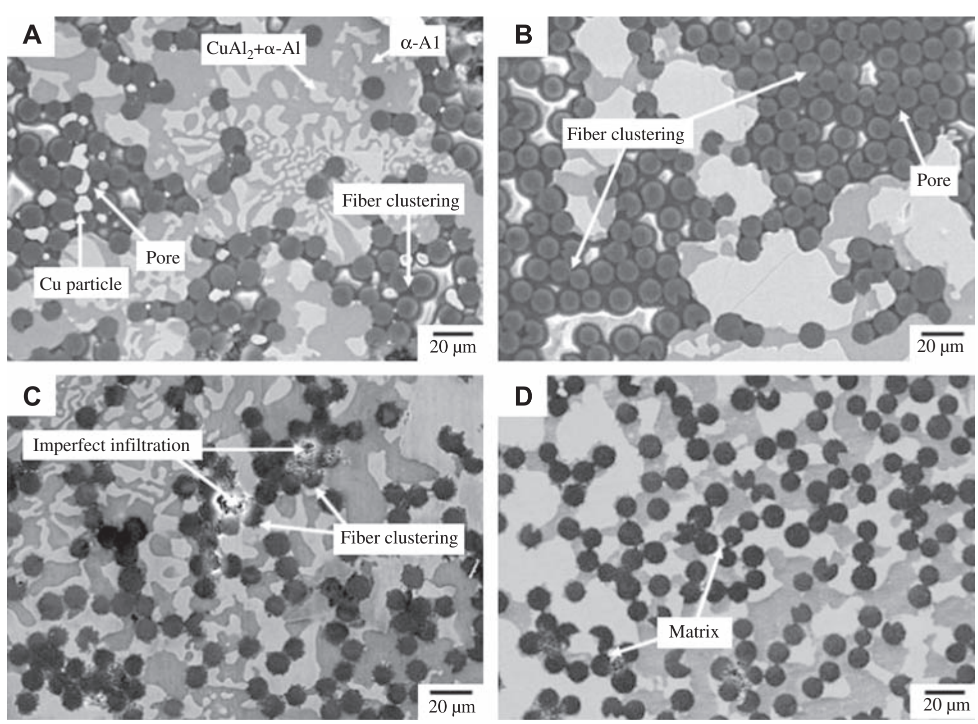

Figure 5 Microstructure of CF/Al composites depending on the added average Cu particles size of; (A) 2.55 μm, (B) 28.86 μm, (C) 11.79 μm and (D) bimodal Cu particles, respectively.

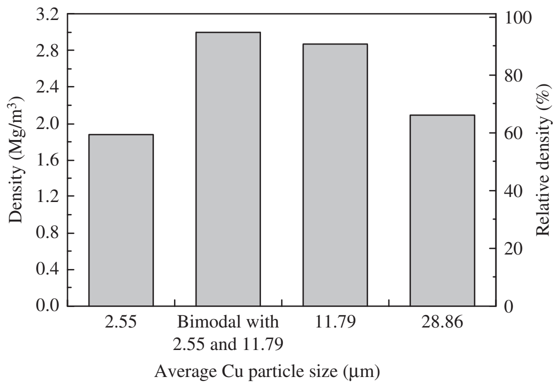

Figure 6 Effect of the added Cu particle sizes on the density of CF/Al composites.

were 1.88, 2.86, 2.09 and 3.00 Mg/m^3 in accordance with the addition of the average Cu particle sizes of 2.55, 11.79, 28.86 μm and bimodal Cu particles, respectively. Especially, CF/Al composites into which were added the bimodal Cu particles, have a high density level corresponding to about 95% of relative density with the nearly homogeneous fiber distribution in the microstructure. In other words, the degradation of the density property of CF/Al composites was significantly influenced on the formation of fiber clustering.

4. Conclusions

1. The added Cu particles to a CF preform were transformed to the deposited particles on CFs and bridging particles between CFs by the SPS process.
2. The compression strength of CF preform increased with the increase of the CF-Cu contact, in accordance with the elevation of the sintering temperature.
3. The density of CF/Al composites improved with increase of the applied infiltration pressure.
4. The addition of smaller or larger particles than the theoretical size for the CF preform, has an adverse effect on homogeneity of the fiber distribution and densification of CF/Al composites.
5. The CF/Al composites into which are added the bimodal Cu particles with average particle sizes of 2.55 μm and 11.79 μm, represented nearly homogeneous fiber array with an excellent relative density of about 95%.

Acknowledgments

This study was supported by the light metal educational foundation in Japan and Grand-in-Aid for Scientific Research (c) [21560771] from the Ministry of Education, Culture, Sports, Science and Technology, Japan and the high technological research project on "Research and Development Center for Advanced Composite Materials" of Doshisha University and Ministry of Education, Culture, Sports, Science and Technology, Japan.

References

[1] Zweben C. *Proc. Of SPIE* 2004, 5530, 194–206.
[2] Januszewski S, Kocizewska-Szczerbik M, Swiatek H. *Microelectron. Reliab.* 1998, 38, 1325–1330.
[3] Azzopardi S, Benmansour A, Ishiko M, Woirgard E. *Microelectron. Reliab.* 2005, 45, 1700–1705.
[4] Ciappa M, Fichtner W, Kojima T, Yamada Y, Nishibe Y. *Microelectron. Reliab.* 2005, 45, 1694–1699.
[5] Dupont L, Lefebvre S, Bouaroudj M, Khatir Z, Faugièrs JC. *Microelectron. Reliab.* 2007, 47, 1767–1772.
[6] Zweben C. *JOM* 1998, 50, 47–51.
[7] Jin S. *JOM* 1998, 50, 46.
[8] Molina JM, Prieto R, Narciso J, Louis E. *Scripta Mater.* 2009, 60, 582–585.
[9] Hanada K, Matsuzaki K, Sano T. *J. Mater. Proc. Tech.* 2004, 153–154, 514–518.
[10] Clyne TW, Mason JF. *Metall. Trans. A* 1987, 18, 1519–1530.
[11] Carreño-Morelli E, Cutard T, Schaller R, Bonjour C. *Mater. Sci. Eng. A* 1998, 251, 48–57.
[12] Choi YB, Sasaki G, Matsugi K, Yanagisawa O. *Mater. Trans.* 2005, 46, 2156–2158.
[13] Choi YB, Matsugi K, Sasaki G, Arita K, Yanagisawa O. *Mater. Trans.* 2006, 47, 1227–1231.
[14] Matsugi K, Kuramoto H, Yanagisawa O, Kiritani M. *Mater. Sci. Eng. A* 2003, 350, 184–189.
[15] Anselmi-Tamburini U, Gennari S, Garay JE, Munir ZA. *Mater. Sci. Eng. A* 2005, 394, 139–148.
[16] Long S, Zhang Z, Flower HM. *Acta Metall. Mater.* 1994, 42, 1389–1397.
[17] Zhang Z, Long S, Flower HM. *Composites* 1995, 25, 380–392.
[18] Mizumoto M, Kaneko Y, Kagawa A. *J. Jpn. I. Met.* 2004, 68, 1047–1052.